A FINITE ELEMENT APPROACH TO THE PRICING OF DISCRETE LOOKBACKS WITH STOCHASTIC VOLATILITY

P.A. FORSYTH*, K.R. VETZAL† AND R. ZVAN‡

Abstract. Finite element methods are described for valuing lookback options under stochastic volatility. Particular attention is paid to the method for handling the boundary equations. For some boundaries, the equations reduce to first order hyperbolic equations which must be discretized to ensure that outgoing waves are correctly modelled. Some example computations show that for certain choices of parameters, the option price computed for a lookback under stochastic volatility can differ from the price under the usual constant volatility assumption by as much as 35% (i.e. \$7.30 compared with \$5.45 for an at-the-money put), even though the models are calibrated so as to produce exactly the same price for an at-the-money vanilla European option with the same time remaining until expiry.

Keywords: Finite element, lookback, stochastic volatility
Running Title: Discrete Lookbacks With Stochastic Volatility
Acknowledgment: This work was supported by the National Sciences and Engineering Research Council of Canada, and the Information Technology Research Center, funded by the Province of Ontario.
Last Revised: July 11, 1997

Contact Address
Peter Forsyth
Department of Computer Science
University of Waterloo
Waterloo Ontario N2L 3G1
email: paforsy@yoho.uwaterloo.ca
Fax: (519) 885-1208
Voice: (519) 888-4567 x4415

* Department of Computer Science, University of Waterloo, Waterloo, Ontario, Canada N2L 3G1, paforsyt@yoho.uwaterloo.ca
† Centre for Advanced Studies in Finance, University of Waterloo, kvetzal@watarts.uwaterloo.ca
‡ Department of Computer Science, University of Waterloo, rzvan@yoho.uwaterloo.ca

1. Introduction. Over the past few years there has been considerable interest in the development of option pricing models which incorporate stochastic volatility. The motivation for this stems from at least two sources. First, empirical evidence supporting the hypothesis of random volatility has been found for a variety of financial time series (e.g. [36] for equities, [29] for foreign currencies, [2, 35] for interest rates). Second, there is evidence of stochastic volatility based on observed option price data. Implied volatilities calculated using the Black-Scholes formula appear to change randomly over time [26]. Moreover, some of the biases of the Black-Scholes model with regard to observed option prices (i.e. the volatility "smile") can be accounted for by stochastic volatility models [9, 1]. One of the conclusions in [1] is that "the amount of persistence in the smile is such that parametric models incorporating long-term memory in stochastic volatility may be the most promising [extension to the Black-Scholes model to explain smile effects]" (p. 24).

A variety of alternative random volatility models have appeared in the literature (e.g. [23, 36, 29, 32, 22, 7, 35]). It is interesting to observe that these have invariably been applied to plain vanilla options. Despite that large and rapidly growing literature dealing with various types of exotic options [28], the issue of the effect of stochastic volatility on the valuation of such options has not been explored (to our knowledge).

In this paper we investigate the pricing of lookback options under stochastic volatility. The terminal payoff of a lookback is a function of the maximum or minimum price reached by the underlying asset over some time period. Closed-form solutions for the valuation of such options have been obtained [21, 13] under the assumptions of constant volatility and continuous monitoring of the underlying asset price. In practice, however, monitoring occurs at discrete intervals (e.g. daily or weekly) and this i) can imply significantly lower option values than the analytic formulas produce [6, 11]; and ii) has led to interest in developing numerical pricing schemes. Previous work in this area has been in a constant volatility framework. Most of it has been based on some variant of the binomial model [6, 24, 11, 8], which would appear to be relatively difficult to extend to the case of stochastic volatility. By contrast, a PDE-based approach is described in Chapter 12 of [37]. See [16] for an application of this method involving American-style lookbacks. This setup can be readily generalized, at least in principle, to include a second random volatility factor. However, there are some subtle numerical issues involved.

The first objective of this paper is to introduce a finite element-finite volume method for discretizing the stochastic volatility option pricing PDE for a discrete lookback. The advantages of this discretization approach can be summarized as follows:

- An unstructured grid finite element approach based on triangular elements can be used. In [20], examples are given which demonstrate the utility of being able to insert nodes at arbitrary locations in the computational domain.
- Discretization of any type of second order term, including *cross derivative* terms presents no particular difficulty. As well, there is an established theory of convergence for these methods for irregularly spaced grids [5], and with appropriate node placement, it is possible to produce discrete equations having desirable

properties [17].

- The first order (hyperbolic) term can be isolated and discretized appropriately (also for unstructured grids) with a finite volume technique [3, 18]. It is well known that if the first order term dominates, then spurious oscillations may swamp the solution [27, 12]. For stochastic volatility models, the PDE reduces to first order hyperbolic near one of the boundaries, so this is clearly a concern. A remedy for this problem involves use of upstream methods [12] or more accurate flux limiters [33]. It is also necessary to carefully treat the boundary equations so that outgoing waves are modelled correctly.

The second objective of this article is to determine the effect of a stochastic volatility model on the price for a discrete lookback. Some example computations are given which compare the price of a lookback under random volatility with the same option valued using constant volatility. The latter computation uses the Black-Scholes implied volatility for an at-the-money vanilla European option with the same maturity. That is, we first calculate the price of an at-the-money vanilla European option of a particular maturity under our stochastic volatility model and then compute the implied volatility to match this price for the constant volatility model. We then compare the prices of lookback options of the same maturity as the vanilla option for the two models. For some choices of parameters, the constant volatility lookback price differs significantly from the price computed using stochastic volatility, even though the models have been constrained to produce the same price for a standard European option.

2. Formulation. We shall first review a standard stochastic volatility model, and then extend this to accommodate discrete lookbacks.

2.1. Stochastic Volatility. Consider an option which is a function of the asset price s and the variance v, which evolve according to the specification given in [22]:

$$\begin{aligned} ds &= \mu s dt^* + \sqrt{v} s dz_1 \\ dv &= \kappa(\theta - v)dt^* + \sigma\sqrt{v} dz_2 \end{aligned} \tag{1}$$

where μ is the expected rate of return on s, κ is the speed of reversion parameter for v, θ is the reversion level of v, σ is the "volatility of volatility", z_1, z_2 are Wiener processes with correlation parameter ρ and t^* represents time. Following the usual steps, the following PDE is obtained for the value of an option $W = W(s, v, t^*)$:

$$\frac{vs^2}{2}W_{ss} + \rho\sigma v s W_{sv} + \frac{\sigma^2 v}{2}W_{vv} + rsW_s + (\kappa(\theta - v) - \lambda v)W_v - rW + W_{t^*} = 0 \tag{2}$$

where λ is the market price of volatility risk and r is the risk free rate of interest.

The boundary conditions for this equation can be determined by examining equation (2). Letting $v, s \to 0$ we obtain:

$$\begin{aligned} W_{t^*} + rsW_s + \kappa\theta W_v - rW = 0; \qquad & v \to 0 \\ W_{t^*} + \frac{\sigma^2 v}{2}W_{vv} + (\kappa(\theta - v) - \lambda v)W_v - rW = 0; \qquad & s \to 0. \end{aligned} \tag{3}$$

For $s \to \infty$ we have:

$$W = \begin{cases} s & \text{for a standard call option} \\ 0 & \text{for a standard put option} \end{cases} \quad ; \quad s \to \infty \tag{4}$$

Finally, for $v \to \infty$, noting that $W_v \to 0$, we obtain

$$W_{t^*} + \frac{vs^2}{2} W_{ss} + rsW_s - rW = 0; \quad v \to \infty \tag{5}$$

2.2. Discrete Lookbacks. A modification of the usual stochastic volatility model may be used to model lookback options. As noted previously, most if not all of these contracts feature discrete monitoring, so we concentrate exclusively on this case. In particular, we suppose that the maximum or minimum of the asset price s is observed at discrete times t_i^* during the life of the option. Let

$$J = \begin{cases} \max_i(s(t_i^*)) & \text{for a put} \\ \min_i(s(t_i^*)) & \text{for a call} \end{cases} \tag{6}$$

Following [37], J can be written as:

$$J = \begin{cases} \lim_{n\to\infty} \left[\int_0^{t^*} \sum_i \delta(t' - t_i^*) s^n \, dt' \right]^{1/n} & \text{for a put} \\ \lim_{n\to\infty} \left[\int_0^{t^*} \sum_i \delta(t' - t_i^*) (1/s)^n \, dt' \right]^{-1/n} & \text{for a call} \end{cases} \tag{7}$$

where

$$\begin{aligned} \delta &= \text{delta function} \\ t_i^* &= \text{lookback observation times} \end{aligned}$$

From equation (7) we can see that:

$$\frac{dJ}{dt^*} = \begin{cases} \lim_{n\to\infty} \left(\frac{1}{n} \sum_i \frac{s^n}{J^{n-1}} \delta(t^* - t_i^*) \right) & \text{for a put} \\ \lim_{n\to\infty} \left(\frac{-1}{n} \sum_i \frac{J^{n+1}}{s^n} \delta(t^* - t_i^*) \right) & \text{for a call} \end{cases} \tag{8}$$

In general, the value of a lookback option with stochastic volatility will be $W = W(J, s, v, t^*)$, i.e. a function of three variables and time. Following [37], the equation for W is given by:

$$\begin{aligned} &\frac{vs^2}{2} W_{ss} + \rho\sigma v s W_{sv} + \frac{\sigma^2 v}{2} W_{vv} + rsW_s + (\kappa(\theta - v) - \lambda v) W_v \\ &-rW + W_{t^*} + \frac{dJ}{dt^*} W_J = 0 \end{aligned} \tag{9}$$

It is convenient to convert equation (9) into an equation forward in time by substituting $t = T - t^*$ where T is the expiry date of the option to give:

$$\begin{aligned} W_t &= \frac{vs^2}{2}W_{ss} + \rho\sigma v s W_{sv} + \frac{\sigma^2 v}{2}W_{vv} + rsW_s + (\kappa(\theta - v) - \lambda v)\, W_v \\ &\quad -rW + \frac{dJ}{dt^*}W_J \end{aligned} \tag{10}$$

where dJ/dt^* can be written in terms of $t = T - t^*$

$$\frac{dJ}{dt^*} = \begin{cases} \lim_{n\to\infty}\left(\frac{1}{n}\sum_i \frac{s^n}{J^{n-1}}\delta(t - t_i)\right) & \text{for a put} \\ \lim_{n\to\infty}\left(\frac{-1}{n}\sum_i \frac{J^{n+1}}{s^n}\delta(t - t_i)\right) & \text{for a call} \end{cases} \tag{11}$$

Note that term $\frac{dJ}{dt^*}W_J$ in equation (10) is zero except at $t = t_i$. As $t \to t_i$, equation (10) becomes:

$$W_t - \frac{dJ}{dt^*}W_J \simeq 0 \tag{12}$$

with the other terms in equation (10) becoming negligible. (Alternatively, one can imagine integrating both sides of equation (10) with respect to time from $t_i - \epsilon$ to $t_i + \epsilon$.) If t^- and t^+ are the times just before and after an observation date t_i, then noting that W is constant along a characteristic, and taking limits as $n \to \infty$, we get the following jump conditions:

$$W(J_+, s, v, t^+) = W(J_-, s, v, t^-) \tag{13}$$

where for a put

$$J_- = \begin{cases} J_+ & \text{if} \quad \frac{J_+}{s} > 1 \\ s & \text{if} \quad \frac{J_+}{s} < 1 \end{cases} \tag{14}$$

and for a call

$$J_- = \begin{cases} J_+ & \text{if} \quad \frac{J_+}{s} < 1 \\ s & \text{if} \quad \frac{J_+}{s} > 1 \end{cases} \tag{15}$$

If the terminal payoff for the lookback has the form

$$\begin{aligned} &\max(J - s, 0) \qquad \text{for a put} \\ &\max(s - J, 0) \qquad \text{for a call} \end{aligned} \tag{16}$$

then a similarity transformation (see [37]) may be used to reduce equation (10) into an equation with two space-like variables and time. If we define

$$\begin{aligned} \alpha &= s/J \\ W(J, s, v, t) &= JU(\alpha, v, t) \end{aligned} \tag{17}$$

then equation (10) becomes simply (at $t \neq t_i$)

$$U_t = \frac{v\alpha^2}{2} U_{\alpha\alpha} + \rho\sigma v\alpha U_{\alpha v} + \frac{\sigma^2 v}{2} U_{vv} + r\alpha U_\alpha + (\kappa(\theta - v) - \lambda v)\, U_v - rU. \tag{18}$$

Note that equation (18) is written for times away from observation times. The boundary conditions are:

$$U_t = r\alpha U_\alpha + \kappa\theta U_v - rU; \qquad v \to 0$$

$$U_t = \frac{\sigma^2 v}{2} U_{vv} + (\kappa(\theta - v) - \lambda v) U_v - rU; \qquad \alpha \to 0 \tag{19}$$

Finally, for $v \to \infty$, noting that the option must become independent of v and that therefore $U_v \to 0$, we obtain

$$U_t = \frac{v\alpha^2}{2} U_{\alpha\alpha} + r\alpha U_\alpha - rU; \quad v \to \infty \tag{20}$$

At $t = 0$ the boundary conditions at $\alpha \to \infty$ are determined from the payoff condition (16)

$$U = \begin{cases} \alpha & \text{for a call} \\ 0 & \text{for a put} \end{cases} \tag{21}$$

At observation times t_i, the following jump conditions must be satisfied (let t^+ and t^- be the times just before and after the observation times). The condition for a put is

$$U(\alpha, v, t^+) = \begin{cases} U(\alpha, v, t^-) & \alpha < 1 \\ \alpha U(1, v, t^-) & \alpha \geq 1 \end{cases} \tag{22}$$

and for a call

$$U(\alpha, v, t^+) = \begin{cases} U(\alpha, v, t^-) & \alpha > 1 \\ \alpha U(1, v, t^-) & \alpha \leq 1 \end{cases} \tag{23}$$

Note that after the first observation times, the boundary conditions as $\alpha \to \infty$ are determined by equations (22, 23).

2.3. Standard Form. In order to discretize equation (18) using a finite element approach, it is convenient to write this equation as:

$$U_t + \mathbf{V} \cdot \nabla U = \nabla \cdot \mathbf{D} \cdot \nabla U - rU \tag{24}$$

where:

$$\mathbf{D} = \frac{1}{2} \begin{pmatrix} v\alpha^2 & \rho\sigma\alpha v \\ \rho\sigma\alpha v & \sigma^2 v \end{pmatrix} \tag{25}$$

and

$$\mathbf{V} = -\begin{pmatrix} r\alpha - v\alpha - \rho\sigma\alpha/2 \\ \kappa(\theta - v) - \lambda v - \sigma^2/2 - \rho\sigma v/2 \end{pmatrix}. \tag{26}$$

Equation (24) has the familiar form of the convection-diffusion equation. A simple physical analogue of equation (24) is a chemical with concentration U being transported by a fluid moving with velocity $\mathbf{V}$, and diffused by diffusion $\mathbf{D}$. If the fluid velocity is large compared to the diffusion, then equation (24) is said to be convection dominated, and behaves numerically like a first order hyperbolic PDE.

3. Discretization. We will now discretize equation (24) using a Galerkin finite element method. In general, the diffusion term in equation (24) can be discretized using standard methods. The convection term in equation (24) can cause difficulties. If the convective term is large compared to the diffusion term, then equation (24) behaves numerically like a hyperbolic equation, and therefore care has to be taken with this term, otherwise spurious oscillations may occur in the discrete solution [10, 38, 12]. Note that boundary equation (19) ($v \to 0$) is first order hyperbolic, and hence care must be taken to ensure that the problem is properly posed at the boundary. Consequently, we will discretize the convective term using a finite volume approach. Formally, a finite volume discretization can be considered to be a Galerkin method with a special quadrature rule [17, 3, 19]. However, it is more intuitively appealing to use a geometric approach for discretizing the convective term.

Consider a discrete two dimensional computational domain R which is tiled by triangles. Let N_i be the usual C^0 Lagrange basis functions defined on triangles. Then,

$$\begin{aligned} N_i &= 1 \text{ at node } i \\ &= 0 \text{ at all other nodes} \\ \sum_j N_j &= 1 \text{ everywhere in the solution domain.} \end{aligned} \tag{27}$$

If $U^n = \sum_j U_j^n$ where $U_j^n = U(\alpha_j, v_j, t^n)$ is the value of U at (α_j, v_j, t^n), then the discretization of equation (24) is given by:

$$\begin{aligned} A_i\left(\frac{U_i^{n+1} - U_i^n}{\Delta t}\right) &= (1-\beta)\left(\sum_{j\in\eta_i}\gamma_{ij}(U_j^{n+1} - U_i^{n+1}) + \sum_{j\in\eta_i}\vec{L_{ij}}\cdot\mathbf{V}_i U_{ij+1/2}^{n+1} - A_i r U_i^{n+1}\right) \\ &\quad +\beta\left(\sum_{j\in\eta_i}\gamma_{ij}(U_j^{n} - U_i^{n}) + \sum_{j\in\eta_i}\vec{L_{ij}}\cdot\mathbf{V}_i U_{ij+1/2}^{n} - A_i r U_i^{n}\right) \\ &\quad +(1-\beta)q_i^{n+1} + \beta q_i^n \end{aligned} \tag{28}$$

where:

$$A_i = \int N_i dR$$

$$
\begin{aligned}
\Delta t &= \text{timestep} \\
\beta &= \text{timeweighting} \\
&\quad \beta = 0 \text{ fully implicit} \\
&\quad \beta = 1 \text{ explicit} \\
&\quad \beta = 1/2 \text{ Crank-Nicolson} \\
U_i^{n+1} &= U(s_i, v_i, t^{n+1}) \\
\gamma_{ij} &= -\int_R \nabla N_i \cdot \mathbf{D} \cdot \nabla N_j dR \qquad (29) \\
\eta_i &= \text{set of neighbours of node } i \\
q_i &= \text{source/sink term used for boundary conditions} \\
U_{ij+1/2}^{n+1} &= \text{value of } U \text{ at the face between} \\
&\quad \text{node } i \text{ and node } j
\end{aligned}
\qquad (30)
$$

We have also used mass lumping for the time derivative term. Other details concerning this discretization method can be found in [17, 20]. Note that A_i can be considered to be the area of the *cell* or finite volume surrounding node i. The finite volume surrounding node i is shown in Figure 1. The finite volume is constructed by joining the midpoint of each edge of a triangle to the centroid of the triangle [3, 25, 18]. The vector length $\vec{L_{ij}}$ in equation (28) is given by

$$\vec{L_{ij}} = \int_a^b \hat{n} ds \qquad (31)$$

where the points a, b are shown in Figure 1, and $\hat{n}$ is the inward pointing normal to the face between node i and node j.

There are various choices for the terms $U_{ij+1/2}$, For example, second order central weighting for $U_{ij+1/2}$ is given by:

$$U_{ij+1/2} = \frac{U_i + U_j}{2} \qquad (32)$$

However, central weighting is prone to producing spurious oscillations [12, 38]. An alternative is first order upstream weighting [12] which is given by

$$
\begin{aligned}
U_{ij+1/2} &= U_i \text{ if } \vec{L_{ij}} \cdot \mathbf{V}_i < 0 \\
&= U_j \text{ otherwise}
\end{aligned}
\qquad (33)
$$

First order upstream weighting is usually too diffusive for accurate solutions. Recently, non-linear flux limiters have been used to obtain accurate solutions without causing oscillations. Essentially, these methods use a more accurate (usually second order) method as much as possible, but reduce to lower order accuracy only where necessary to avoid spurious oscillations [38, 39]. One popular method uses a van Leer limiter [33, 27, 10]. With reference to Figure 1, assume that node i is upstream of node

FIG. 1. *Finite volume surrounding node i. Points a and b are the centroids of their respective triangles. The line segments from a and b pass through the midpoint of the triangle edge $i-j$.*

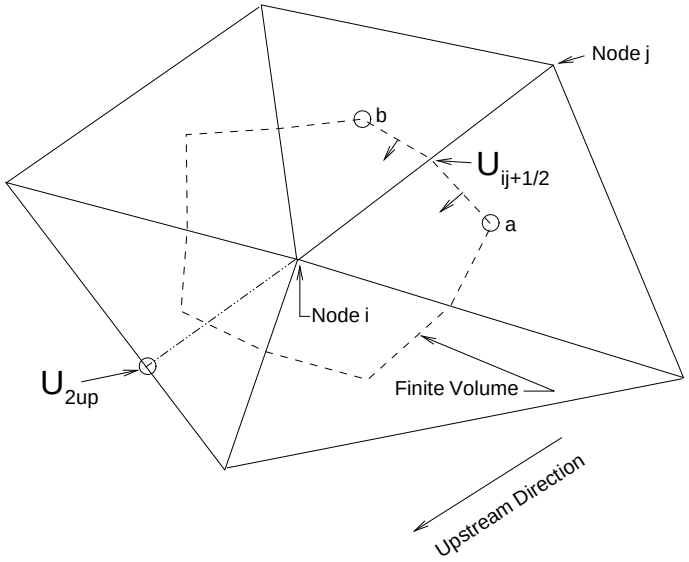

j (the upstream directions are given by equation (33)). Point $2up$ is the value of U which is upstream of node i, interpolated using the two nearest nodes where U is known (see Figure 1). In this case,

$$U_{ij+1/2} = U_i + \sigma(r_{ij}) \left(\frac{U_j - U_i}{2} \right) \tag{34}$$

where

$$r_{ij} = \frac{\dfrac{U_i - U_{2up}}{\|\mathbf{x}_i - \mathbf{x}_{2up}\|}}{\dfrac{U_j - U_i}{\|\mathbf{x}_j - \mathbf{x}_i\|}}. \tag{35}$$

where the van Leer limiter [33] is defined by

$$\begin{aligned} \sigma(r) &= 0\ , \quad \text{if} \quad r \leq 0 \\ &= \frac{2r}{1+r}\ , \quad \text{if} \quad r > 0. \end{aligned} \tag{36}$$

and $\mathbf{x}_i$ is the location vector of node i. Other possibilities include the smooth MUSCL limiter described in [4].

A van Leer limiter can be shown to be TVD (total variation diminishing) in one dimension. This is a formal specification of an oscillation free solution [27].

FIG. 2. *Finite volume surrounding node i at the boundary. Point m is in the interior of the computational domain. Line im is perpendicular to $k^- k^+$.*

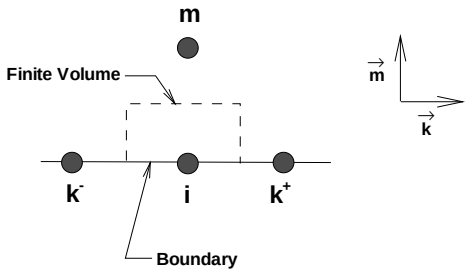

4. Discretization of Boundary Conditions. Equations (28) are used for all interior points in the computational domain. For nodes on the boundary, the discrete equations can be deduced from the boundary equations (19-20). Note that the discrete equations (28) are valid for a completely unstructured grid. Some examples showing the utility of being able to insert nodes near points of interest is given in [20]. However, in order to construct discrete boundary equations having a simple form, it is advantageous to ensure that the grid is unstructured except for the following constraint: for any node i on the boundary, there exists a (nearby) node m in the interior of the computational domain such that the line im is perpendicular to the boundary. It is easy to construct such a grid, given an arbitrary grid, by inserting some extra nodes if necessary. If the grid satisfies this condition, then a straightforward finite volume approach can be used to discretize equations (19-20).

Consider a node i on the boundary, as depicted in Figure 2. Let $\hat{k}$ be the unit vector pointing along the boundary, and let $\hat{m}$ be a unit vector perpendicular to the boundary pointing inward to the computational domain.

If $\mathbf{x}_i$ is the location vector of node i, then let

$$\begin{aligned} \Delta x_{ik^-} &= \|\mathbf{x}_i - \mathbf{x}_{k^-}\| \\ \Delta x_{ik^+} &= \|\mathbf{x}_i - \mathbf{x}_{k^+}\| \\ \Delta x_{im} &= \|\mathbf{x}_i - \mathbf{x}_m\| \end{aligned} \tag{37}$$

The finite volume discretization of equations (19-20) then has the same form as the discrete equations (28), if we define the various terms appropriately. Let:

$$\begin{aligned} \vec{L_{ik^-}} &= \frac{\Delta x_{im}}{2}\hat{k} \\ \vec{L_{ik^+}} &= -\frac{\Delta x_{im}}{2}\hat{k} \end{aligned}$$

TABLE 1
Definition of terms in equation (28) for boundary nodes.

$v \to 0$	
$\mathbf{V}_i$	$-r\alpha_i\hat{k} - \kappa\theta\hat{m}$
q_i^{n+1}	$-\|\vec{L_{im}}\|\kappa\theta U_i^{n+1}$
$\gamma_{ik}(k = k^+, k^-)$	0
$\alpha \to 0$	
$\mathbf{V}_i$	$(-\kappa(\theta - v_i) + \lambda v_i)\,\hat{k}$
q_i^{n+1}	0
$\gamma_{ik}(k = k^+, k^-)$	$T_{ik}\sigma^2 v_i/2$
$v \to \infty$	
$\mathbf{V}_i$	$-r\alpha_i\hat{k}$
q_i^{n+1}	0
$\gamma_{ik}(k = k^+, k^-)$	$T_{ik}\alpha_i^2 v_i/2$

$$
\begin{aligned}
\vec{L_{im}} &= -\left(\frac{\Delta x_{ik^+} + \Delta x_{ik^-}}{2}\right)\hat{m} \\
A_i &= \left(\frac{\Delta x_{im}}{2}\right)\left(\frac{\Delta x_{ik^+} + \Delta x_{ik^-}}{2}\right) \\
T_{ik^-} &= \frac{\Delta x_{im}}{2}/\Delta x_{ik^-} \\
T_{ik^+} &= \frac{\Delta x_{im}}{2}/\Delta x_{ik^+} \\
\eta_i &= \{k^-, k^+, m\} \\
\gamma_{im} &= 0
\end{aligned}
\tag{38}
$$

Table 4 shows the definitions of the remaining terms in equation (28) for the boundary nodes for each of the cases in equations (19-20).

Note that for the case $v \to 0$ in Table 4 we have assumed that $\vec{L_{im}} \cdot \mathbf{V}_i \geq 0$ (in equation (28)). This means that the domain of dependence of a point on the boundary consists of points interior to the computational domain, and other points on the boundary. The non-zero source term for this case ($v \to 0$) accounts for the first order hyperbolic term which results in outgoing waves [3].

It is now clear why we used the original boundary equations (19-20) instead of taking the limit as (say) $v \to 0$ in equation (26). For example, if $v \to 0$ in equation

(26), then we obtain

$$\mathbf{V} = \begin{pmatrix} -r\alpha + \rho\sigma\alpha/2 \\ -\kappa\theta + \sigma^2/2 \end{pmatrix}. \tag{39}$$

In this case, the component of velocity normal to the boundary from equation (39) is $(-\kappa\theta + \sigma^2/2)\,\hat{v}$, may not always point in the negative $\hat{v}$ direction. This would cause some complication, since we know that no boundary data exterior to the domain should be required.

Boundary conditions as $\alpha \to \infty$ are simple Dirichlet conditions. Initially, conditions (21) are applied, which may be altered at observation times.

Immediately after each observation times, the jump conditions (13-15) are imposed by using linear interpolation on each triangle (the finite element basis functions are conveniently available for this purpose). The determination of the appropriate triangle to be used in the interpolation is based on a fast point location algorithm which uses the finite element basis functions [30].

5. Solution of the discrete equations. The discrete equations (28) are in general non-linear. This is due to the use of a nonlinear flux limiter for the convection term. Nonlinearities are also introduced if the American early exercise constraint is applied [20]. Consequently, an approximate Newton iteration will be used to solve the discrete equations. The complete Jacobian is constructed with the exception of all derivatives with respect to the the second upstream points U_{2up} (in equation 35), which are ignored. The iteration for a given timestep is deemed to have converged when

$$\max_i |(U_i^{n+1})^{k+1} - (U_i^{n+1})^k| < tol \tag{40}$$

where $(U_i^{n+1})^k$ is the k^{th} iterate for U_i^{n+1}.

Note that if a direct method is used to solve the Jacobian, then implicit methods can be very expensive in two or more dimensions. For example, in [16], a band solver was used to solve the matrix. However, modern sparse matrix iterative methods are very efficient at solving problems generated by PDE timestepping, since a good initial guess (from the previous timestep) is available. In this study, the Jacobian is solved using an incomplete LU [14, 15] preconditioned CGSTAB iteration [34]. This method is completely general, and makes no assumptions about the structure of the sparse matrix.

An automatic timestep selection method is also used [31].

6. Example Computations. In order to validate our lookback model, we set $\kappa = \rho = \sigma = \lambda = 0$ in equation (18). The solution of this model for a given value of $v = (volatility)^2$ will then correspond to a lookback with a constant volatility. Using the parameters $r = .1$, $v = .04$, and time to expiry of one year, with observation times $.5, 1.5, 2.5, \ldots, 11.5$ months, this corresponds to the case given in [37].

This problem was run on a grid with various numbers of nodes in the s/J direction, where J is maximum observed asset price for a put. At each grid refinement, the

TABLE 2

Comparison of discrete lookback put with constant volatility with the results in [37]. Value given as for $U = W/J$ (see equation 17). Grid size given as total number of nodes in the s/J direction.

	This work		
Grid Size	$s/J = .9$	$s/J = 1.0$	$s/J = 1.1$
93	.09999	.08863	.09525
185	.10020	.08883	.09545
389	.10025	.08885	.09546
	Results from [37]		
Not Stated	.101	.089	.095

TABLE 3

Common data for the stochastic volatility lookback cases.

θ	.04
λ	0.0
r	.10
Time to expiry	0.5 years
Observation times	Weekly
	(1/52 of a year)

timestep parameters were also reduced. Table 2 compares our results with those from [37].

In order to analyze the effect of stochastic volatility on lookback options, we calculated lookback values under both constant and random volatility for several cases. The volatility parameter for the constant volatility models was determined by first computing the price of an at-the-money European vanilla call option with 0.5 years remaining until expiry for the stochastic volatility case at hand and then finding the Black-Scholes implied volatility for this option value. Note that this means that our constant and stochastic volatility specifications were constrained to produce exactly the same price for a standard European call option (and, by put-call parity, exactly the same price for a standard European put option as well). All cases used the common parameters in Table 3. The other data for the four cases is given in Table 4, including the computed implied volatilities.

Figure 3 shows the value of a lookback put computed using the stochastic volatility model given by equation (18). The values shown are actually $U = W/J$, where W is actual value of the option, and J is the most recently observed maximum of the

TABLE 4
Data for the stochastic volatility lookback cases.

Case	κ	σ	ρ	B-S implied volatility
1	.2	.5	.5	16.72%
2	.2	.5	-.5	19.27%
3	2.0	.2	.5	19.43%
4	2.0	.2	-.5	20.17%

TABLE 5
Convergence of constant volatility lookback. A value of $v = .04$ (volatility $= .2$) was used. Grid size is given as the number of points in the s direction. Value given as for $W = JU$ for $J = 100$.

	Put		
Grid Size	$s/J = .9$	$s/J = 1.0$	$s/J = 1.1$
160	9.68	7.66	8.28
320	9.68	7.65	8.27
	Call		
160	10.43	11.88	17.03
320	10.43	11.88	17.03

asset price. The parameters are given in Table 3 and Case 1, Table 4. This Figure clearly shows the local minimum in the value of the put (along lines of constant v) near $s/J = 1$. In contrast, Figure 4 shows the contours for the lookback call, Case 1, for the same data. Note that the put shows a more complex behaviour as a function of v than the call, and hence we can expect a greater diffusion effect in the v direction for the put. Not surprisingly, the figures also demonstrate that option values can be quite different when the initial level of v is not equal to its long run mean level of .04.

Table 5 illustrates the convergence of our algorithm in the constant volatility case where $v = .04$ (corresponding to a constant volatility of .20). The timestepping parameters were adjusted so that there was no change to four significant figures.

Table 5 indicates that the results with 320 nodes in the s/J direction are accurate to within \$0.01. The above runs were repeated using this grid for all the implied volatilities given in Table 4. The results are given in Table 6.

The full stochastic volatility lookback model was run for all 4 cases. Two grids, with $19,551$ nodes and $77,645$ nodes were used, in order to check the solution accuracy. The worst case (in terms of solution accuracy) was Case 2, which is shown in Table

FIG. 3. *Stochastic volatility lookback put. Contours of* $U = W/J$, *where* $J = \max_i S(t_i)$ *shown. Data are for Case 1, Table 4, weekly observation.*

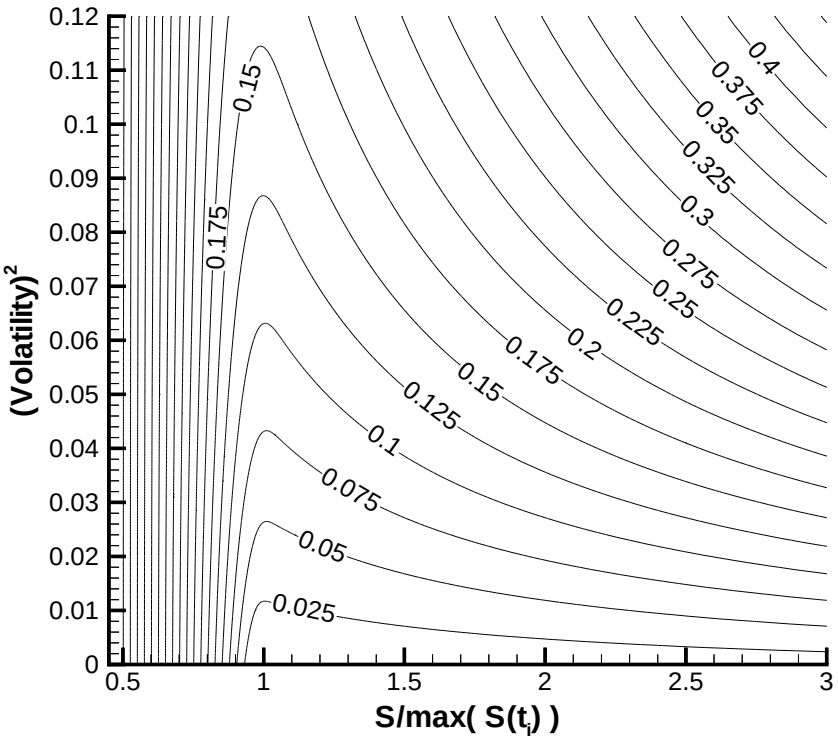

FIG. 4. *Stochastic volatility lookback call. Contours of* $U = W/J$, *where* $J = \min_i S(t_i)$ *shown. Data are for Case 1, Table 4, weekly observation.*

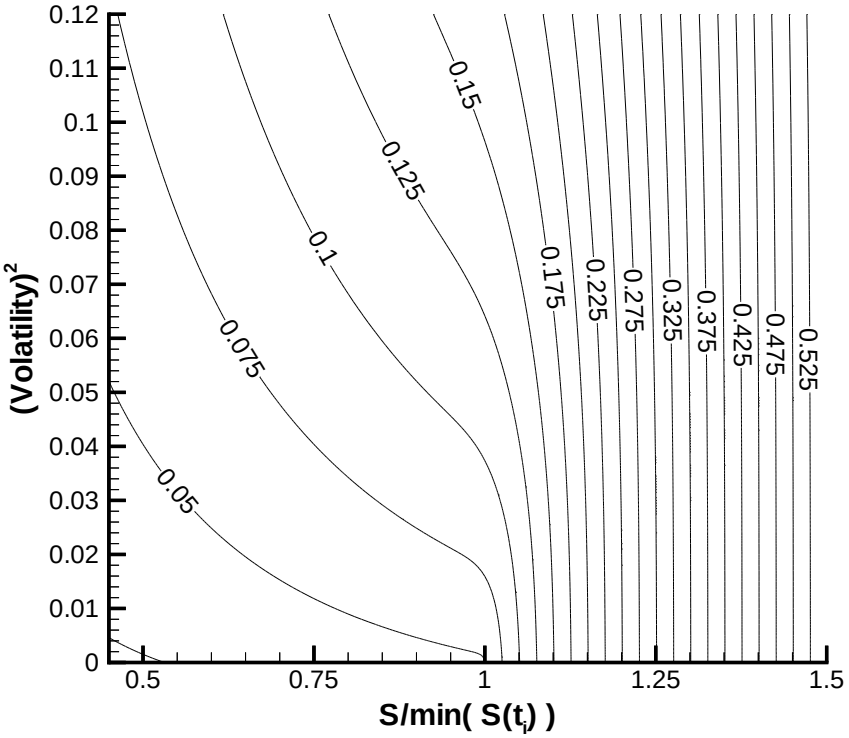

TABLE 6

Values of a constant volatility lookback, for the values of the Black-Scholes implied volatilities given in Table 4. Results are correct to within .01. Value given for $W = JU$ for $J = 100$. Compare with Table 8.

Case	$s/J = .9$	$s/J = 1.0$	$s/J = 1.1$
	Put		
1	8.42	6.05	6.54
2	9.39	7.30	7.89
3	9.46	7.38	7.97
4	9.75	7.75	8.37
	Call		
1	9.18	10.47	16.11
2	10.16	11.57	16.82
3	10.22	11.64	16.86
4	10.50	11.96	17.09

7. Reduction in the timestepping parameters showed no change in the solution to four figures. The results indicate that the solution error (in the worst case) is about \$0.04. If the error is assumed to be $O(h^2)$ (h being the mesh size parameter [5]), then the actual error for the finest grid is probably about .01.

It is interesting to observe from Tables 6 and 8 that there can be significant differences between the constant and stochastic volatility values, particularly for the puts. For example, under Case 2, the price of the at-the-money put for the stochastic volatility model is \$5.45, compared to \$7.30 for the constant volatility model. This 35% difference is quite significant. Even though the differences for the call options are smaller, it is clear from these two tables that a constant volatility model can be a very poor approximation to the two factor model.

7. Conclusions. In this paper, we have developed a finite element-finite volume method for discretizing the pricing PDE for lookbacks with stochastic volatility. This technique correctly handles the limiting case as $v \to 0$ where the equation becomes first order hyperbolic. As well, the boundary equations are also discretized so that outgoing waves are correctly modelled.

Our illustrative computations demonstrate that the stochastic volatility model can produce lookback values which are significantly different from the constant volatility model, even though the two models are calibrated to generate the same price for a standard European option of the same maturity. This suggests a need for further research into the effects of stochastic volatility on the valuation of various types of

TABLE 7

Convergence of the stochastic volatility lookback option for Case 2. Value given as for $W = JU$ for $J = 100$. Grid size given as total number of nodes.

	Put		
Grid Size	$s/J = .9$	$s/J = 1.0$	$s/J = 1.1$
19,551	7.87	5.41	5.80
77,645	7.88	5.45	5.84
	Call		
19,551	10.38	11.98	17.91
77,645	10.37	11.95	17.90

TABLE 8

Values of a discrete stochastic volatility lookback. Results are correct to within .04 in the worst case. Value given for $W = JU$ for $J = 100$. Compare with Table 6.

Case	$s/J = .9$	$s/J = 1.0$	$s/J = 1.1$
	Put		
1	10.16	7.07	7.56
2	7.88	5.45	5.84
3	9.99	7.82	8.44
4	9.22	7.23	7.80
	Call		
1	8.97	10.27	16.06
2	10.36	11.95	17.90
3	10.06	11.46	16.61
4	10.60	12.09	17.40

exotic options. We conjecture that similar effects might well be observed, for example, in the case of barrier options.

REFERENCES

[1] Y. Aït-Sahalia and A.W. Lo. Nonparametric estimation of state-price densities implicit in financial asset prices. Working paper, University of Chicago and M.I.T., 1997.

[2] T.G. Anderson and J. Lund. Estimating continuous time stochastic volatility models of the short term interest rate. *J. Econometrics*, 77:343–377, 1997.

[3] W.K. Anderson and D.L. Bonhaus. An implicit upwind algorithm for computing turbulent flows on unstructured grids. *Comp. Fluids*, 23:1–25, 1994.

[4] W.K. Anderson, J.L. Thomas, and B. Van Leer. Comparison of finite volume flux vector splittings for the Euler equations. *AIAA J.*, 24:1453–1460, 1986.

[5] O. Axellson and V. Barker. *Finite Element Solution of Boundary Value Problems.* Academic Press, 1984.

[6] S. Babbs. Binomial valuation of lookback options. Working paper, Midland Montagu, Capital Markets, London, 1992.

[7] C.A. Ball and A. Roma. Stochastic volatility option pricing. *J. Fin. Quant. Anal.*, 29:589–607, 1994.

[8] J. Barraquand and T. Pudet. Pricing of American path-dependent contingent claims. *Math. Fin.*, 6:17–51, 1996.

[9] D.S. Bates. Jumps and stochastic volatility: Exchange rate processes implicit in Deutsche mark options. *Rev. Fin. Studies*, 9:69–107, 1996.

[10] M. Blunt and B. Rubin. Implicit flux limiting schemes for petroleum reservoir simulation. *J. Comp. Phys.*, 102:194–210, 1992.

[11] T.H.F. Cheuk and T.C.F. Vorst. Lookback options and the observation frequency: A binomial approach. Working paper, Erasmus University, 1994.

[12] N. Clarke and K. Parrot. The multigrid solution of two factor american put options. Research Report 96-16, Oxford Computing Laboratory, Oxford, 1996.

[13] A. Conze and R. Viswanathan. Path dependent options: The case of lookback options. *J. Finance*, 46:1893–1907, 1991.

[14] E.F. D'Azevedo, P.A. Forsyth, and W.P. Tang. Ordering methods for preconditioned conjugate gradient methods applied to unstructured grid problems. *SIAM J. Matrix Anal. Applic.*, 13:944–961, 1992.

[15] E.F. D'Azevedo, P.A. Forsyth, and W.P. Tang. Towards a cost effective ILU preconditioner with high level fill. *BIT*, 32:442–463, 1992.

[16] M.A.H. Dempster and J.P. Hutton. Fast numerical valuation of American, exotic and complex options. *App. Math. Fin.*, 4:1–20, 1997.

[17] P.A. Forsyth. A control volume finite element approach to NAPL groundwater contamination. *SIAM J. Sci. Stat. Comp.*, 12:1029–1057, 1991.

[18] P.A. Forsyth and H. Jiang. Nonlinear iteration methods for high speed laminar compressible Navier-Stokes equations. *Comp. Fluids*, 26:249–268, 1997.

[19] P.A. Forsyth and M.C. Kropinski. Monotonicity considerations for saturated-unsaturated subsurface flow. *SIAM J. Sci. Comp.*, 1997. to appear.

[20] P.A. Forsyth, R. Zvan, and K. Vetzal. A general finite element approach for PDE option pricing. 1997. Conference on numerical methods in finance, Toronto, 1997.

[21] M.B. Goldman, H.B. Sosin, and M.A. Gatto. Path dependent options: "Buy at the low, sell at the high". *J. Finance*, 34:1111–1127, 1979.

[22] S.L. Heston. A closed form solution for options with stochastic volatility and applications to bond and currency options. *Rev. Fin. Studies*, 6:327–343, 1993.

[23] J. Hull and A. White. The pricing of options on assets with stochastic volatilities. *J. Finance*, 42:281–300, 1987.

[24] J. Hull and A. White. Efficient procedures for valuing European and American path-dependent options. *J. Derivatives*, Fall:21–31, 1993.

[25] H. Jiang and P.A. Forsyth. Robust linear and nonlinear strategies for solution of the transonic Euler equations. *Comp. Fluids*, 24:753–770, 1995.

[26] C.G. Lamoureux and W.D. Lastrapes. Forecasting stock-return variance: Toward an understanding of stochastic implied volatilities. *Rev. Fin. Studies*, 6:293–326, 1993.

[27] R. J. LeVeque. *Numerical Methods for Conservation Laws*. Birkhauser, 1990.

[28] S. Lyden. Reference check: A bibliography of exotic options models. *J. Derivatives*, Fall:79–91, 1996.

[29] A. Melino and S.M. Turnbull. Pricing foreign currency options with stochastic volatility. *J. Econometrics*, 45:239–265, 1990.

[30] J. O'Rourke. *Computational Geometry in C*. Cambridge University Press, 1994.

[31] B. Rubin and P.H. Sammon. Practical control of timestep selection in thermal simulation. *Soc. Pet. Eng. Res. Eng.*, 1:163–170, 1986.

[32] E.M. Stein and J.C. Stein. Stock price distributions with stochastic volatility: An analytical approach. *Rev. Fin. Studies*, 4:727–752, 1991.

[33] P.K. Sweby. High resolution schemes using flux limiters for hyperbolic conservation laws. *SIAM J. Num. Anal.*, 21:995–1011, 1984.

[34] H.A. van der Vorst. Bi-CGSTAB: A fast and smoothly converging variant of Bi-CG for the solution of nonsymmetric linear systems. *SIAM J. Sci. Stat. Comp.*, 13:631–645, 1992.

[35] K.R. Vetzal. Stochastic volatility, movements in short term interest rates, and bond option values. *J. Banking Fin.*, 21:169–196, 1997.

[36] J.B. Wiggins. Option values under stochastic volatility: Theory and empirical estimates. *J. Fin. Econ.*, 19:351–372, 1987.

[37] P. Wilmott, J. Dewynne, and S. Howison. *Option Pricing*. Oxford Financial Press, 1993.

[38] R. Zvan, P.A. Forsyth, and K.R. Vetzal. Robust numerical methods for PDE models of Asian options. 1996. University of Waterloo Department of Computer Science Technical Report CS-96-28, submitted to J. Comp. Fin.

[39] R. Zvan, K.R. Vetzal, and P.A. Forsyth. PDE methods for pricing barrier options. 1997. Conference on numerical methods in finance, Toronto, 1997.